Floating Liquid Phase in Sedimenting Colloid-Polymer Mixtures

Matthias Schmidt,[1,*] Marjolein Dijkstra,[1] and Jean-Pierre Hansen[2,†]

[1]*Soft Condensed Matter, Debye Institute, Utrecht University, Princetonplein 5, 3584 CC Utrecht, The Netherlands*

[2]*Institute for Theoretical Physics, Utrecht University, Leuvenlaan 4, 3584 CE Utrecht, The Netherlands*

(Received 21 January 2004; published 20 August 2004)

Density functional theory and computer simulation are used to investigate sedimentation equilibria of colloid-polymer mixtures within the Asakura-Oosawa-Vrij model of hard sphere colloids and ideal polymers. When the ratio of buoyant masses of the two species is comparable to the ratio of differences in density of the coexisting bulk (colloid) gas and liquid phases, a stable "floating liquid" phase is found, i.e., a thin layer of liquid sandwiched between upper and lower gas phases. The full phase diagram of the mixture under gravity shows coexistence of this floating liquid phase with a single gas phase or a phase involving liquid-gas equilibrium; the phase coexistence lines meet at a triple point. This scenario remains valid for general asymmetric binary mixtures undergoing bulk phase separation.

DOI: 10.1103/PhysRevLett.93.088303 PACS numbers: 83.80.Hj, 64.70.Fx, 82.70.Dd

Equilibrium sedimentation profiles of colloidal dispersions or biomolecular solutions have been extensively measured since the pioneering experiments of Jean Perrin [1], and yield a wealth of information, in particular the osmotic equation of state of the suspension over a wide range of concentrations [2]. Sedimentation equilibria of suspensions involving two or more components often show highly nontrivial behavior, as in the case, e.g., of binary hard sphere colloid mixtures [3], of charged colloidal particles in the presence of a low ionic strength electrolyte [4–6] or of mixtures of colloidal platelets and nonadsorbing polymer [7]. Such multicomponent systems generally undergo a demixing transition in the bulk. Under gravity the density profiles may then cross phase boundaries at well-defined altitudes z, so that the suspension may be expected to segregate into horizontal slabs of different chemical compositions. In this Letter, we demonstrate that two-phase bulk coexistence of any asymmetric binary mixture can give rise to apparent three-phase coexistence in sedimentation equilibrium. A necessary condition is that the mass densities of both phases are equal for at least one single statepoint at bulk coexistence, which can (in principle) be always fulfilled by choosing the mass ratio of both components appropriately. Before arguing that the phenomenon is general, we investigate in detail the particular case of binary mixtures of hard sphere colloids (of diameter σ_c), and of ideal polymer coils (of diameter σ_p). Within the familiar Asakura-Oosawa-Vrij (AOV) [8] model, the latter may freely interpenetrate while their centers are excluded from spheres of radius $(\sigma_c + \sigma_p)/2$ around each colloidal particle. Such highly nonadditive hard core interactions are known to drive a separation into a low colloid concentration "gas" phase and a high concentration colloidal "liquid" phase in the bulk, for size ratios σ_p/σ_c above a threshold value of the order of $1/3$ [9,10].

We consider explicitly the case $\sigma_c = \sigma_p$. If m_i ($i = c$ or p) denotes the buoyant mass of particles of species i, the potential energy of the latter in the gravitational field is $V_i^{\text{ext}}(z) = m_i g z$ for $z > \sigma_i/2$ (the base of the vertical recipient of overall height L is taken to be $z = 0$), where g is the acceleration of gravity. The gravitational lengths associated with the two species are $\xi_i = k_B T/(m_i g)$, where k_B is Boltzmann's constant and T is the absolute temperature. The equilibrium sedimentation profiles of the two species, $\rho_c(z)$ and $\rho_p(z)$, are determined, within density functional theory (DFT), by minimizing the grand potential $\Omega[\rho_c, \rho_p]$ of the inhomogeneous suspension with respect to the profiles $\rho_i(z)$. The functional Ω is conventionally split into ideal, excess and external parts:

$$\Omega[\rho_c, \rho_p] = F_{\text{id}}[\rho_c] + F_{\text{id}}[\rho_p] + F_{\text{exc}}[\rho_c, \rho_p] + \sum_{i=c,p} \int_0^L \rho_i(z)[V_i^{\text{ext}}(z) - \mu_i]dz, \quad (1)$$

where the ideal gas free energy functional is $F_{\text{id}}[\rho_i] = k_B T \int_0^L \rho_i(z)\{\ln[\rho_i(z)\Lambda_i^3] - 1\}dz$. Λ_i is an irrelevant length scale (which will be set equal to σ_i for convenience); μ_i is the chemical potential of species $i = c$ or p. The excess part, F_{exc}, arises from the interactions between the particles in the suspension. If the sedimentation lengths, ξ_i, are appreciably larger than the particle diameters σ_i, i.e., for slowly varying inhomogeneities, the local density approximation (LDA) for F_{exc} is expected to be accurate, except at the bottom of the suspension where layering occurs [11]. Within LDA: $F_{\text{exc}}[\rho_c, \rho_p] = \int_0^L \Phi[\rho_c(z), \rho_p(z)]dz$, where Φ is the bulk Helmholtz free energy density, which is accurately given by free-volume theory for the AOV model [9]. The LDA neglects nonlocal correlations, which are approximately included within the fundamental measure theory (FMT) [12], as adapted to the AOV model [13]. This theory leads back to the free-volume free energy in the homogeneous bulk limit, so that the two DFT treatments that we apply are consistent in this respect.

As a check of the predictions of the DFT calculations, we have also carried out extensive Monte Carlo (MC)

simulations of the same model under identical physical conditions. The simulation cell is of total height $L = 220\sigma_c$ and its square basis of edge length $l = 5\sigma_c$ is periodically repeated in the x and y directions; we checked system size dependence with simulations using $l = 25\sigma_c$ and we found that the sedimentation equilibria are similar within the statistical accuracy.

It is straightforward to show that the slope of the bulk liquid-gas binodal obeys

$$\left.\frac{d\mu_p}{d\mu_c}\right|_{\text{coex}} = -\frac{\Delta\rho_c}{\Delta\rho_p}, \tag{2}$$

where $\Delta\rho_i = \rho_i^l - \rho_i^g$, and ρ_i^g (ρ_i^l) is the density of species $i = c, p$ in the gas (liquid) phase. In the LDA spirit we define a "local" chemical potential $\mu_i(z) = \mu_i - m_i g z$ which describes a linear path, parametrized by z, in the (μ_c, μ_p) representation of the bulk phase diagram. The slope of the path is $d\mu_p/d\mu_c = m_p/m_c$, and one might hence anticipate interesting behavior when this ratio is of the order of the typical slope of the (generally curved [14]) binodal, which implies $m_c\Delta\rho_c \sim -m_p\Delta\rho_p$. Indeed for a size ratio $q = \sigma_p/\sigma_c = 1$, the DFT calculations predict a striking stacking of gas, liquid and gas phases within a limited window of (buoyant) mass ratios m_p/m_c. The density profiles calculated within the FMT version of DFT for $m_p/m_c = 0.235$ are shown in Fig. 1 for four values of the ratio σ_c/ξ_c, and keeping $\mu(z_0) = \text{const}$ at an (arbitrary) reference height, chosen as $z_0 = L/4 = 55\sigma_c$. For the largest value of σ_c/ξ_c, the system is in a colloidal gas phase. As the colloids are about 4 times heavier than the polymer, one would naively expect them to be at the bottom of the container; yet they rather accumulate at high altitudes. For decreasing values of σ_c/ξ_c, we find a novel layered structure of sedimentation profiles: a "floating" liquid slab, containing practically only colloidal particles, is seen to be sandwiched between two polymer rich slabs of gas. The lower slab is practically free of colloids, while the concentration of the latter remains significant in the upper slab. The absence of colloids in the lower slab is again counter intuitive. The interfaces between these three phases are very sharp, particularly at the lower liquid-gas interface, where the colloid density profiles are seen to exhibit some low-amplitude oscillations on the liquid side, representative of weak layering. The width of the floating liquid layer is of the order of 40 colloid diameters, so that it may be regarded as practically bulklike. The corresponding density profiles calculated within the LDA are very similar, but the lower liquid-gas interface is shifted to slightly lower altitudes and the small structure in the colloid profiles is of course suppressed. The inset in Fig. 1 shows that the thermodynamic path followed with increasing altitude indeed crosses the bulk liquid-gas coexistence curve twice, thus leading to the two observed interfaces. Upon increasing z, the sedimentation path crosses first the bulk binodal at large μ_p and μ_c, where

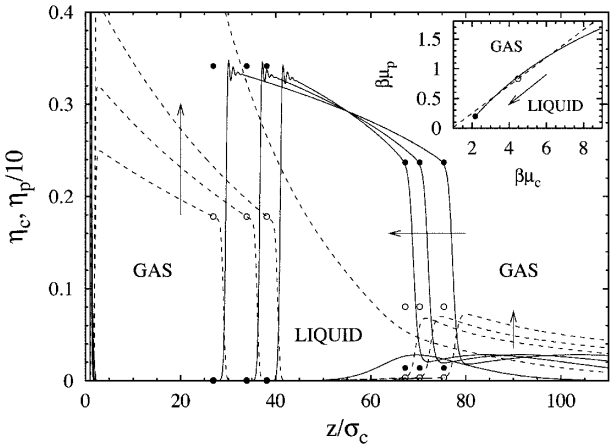

FIG. 1. Scaled density profiles of colloids $\eta_c(z)$ (solid lines) and polymers $\eta_p(z)/10$ (dashed lines) versus scaled height z/σ_c for size ratio $q = \sigma_p/\sigma_c = 1$ and mass ratio $m_p/m_c = 0.235$. Shown are DFT results for statepoint $\beta\mu_c = 4.4794 + \beta m_c g z_0$, $\beta\mu_p = 0.8294 + \beta m_p g z_0$, where $z_0 = 55\sigma_c$, and for increasing gravitational strength $\sigma_c/\xi_c = 0.06, 0.08, 0.1, 0.2$ (indicated by arrows). Also shown are the LDA predictions for the density jumps of colloids (filled circles) and polymers (open circles). The inset shows the fluid part of the bulk phase diagram as a function of the chemical potentials $\beta\mu_c$ and $\beta\mu_p$. The full line is the liquid-gas binodal terminating at a critical point (full circle). The sedimentation path (dashed line) for increasing z (indicated by the arrow) crosses the binodal twice. Also shown is the statepoint (open circle) corresponding to $z = z_0$.

a very dilute colloidal gas coexists with a rather dense colloidal liquid phase, and then crosses the bulk binodal closer to the critical point, where the colloid densities become comparable in the two coexisting phases. This explains why the lower slab is very dilute in colloids, while the upper slab contains more colloids, despite their larger mass. For significantly smaller or larger mass ratios m_p/m_c no, or only one intersection occurs corresponding to a single phase throughout the inhomogeneous colloid-polymer mixture, or to a single interface separating liquid and gas phases, as will be discussed in more detail below.

Three of the corresponding MC-generated profiles are shown in Fig. 2, together with snapshots of typical configurations of the equilibrated binary system. The agreement between DFT results shown in Fig. 1 and simulation results is seen to be quantitative. The mass density profiles (not shown) $\rho_m = m_c\rho_c + m_p\rho_p$ decrease monotonically, except for some oscillations at the lower liquid-gas interface and to a much lesser extent at the upper interface, with z. The rate of decrease is much smaller in the liquid slab, as expected from the lower osmotic compressibility of that phase.

In order to establish a tentative phase diagram for the observed stacked sedimentation, we carried out a semimacroscopic, modified LDA calculation in the spirit of Kelvin's theory of capillary condensation. Depending on

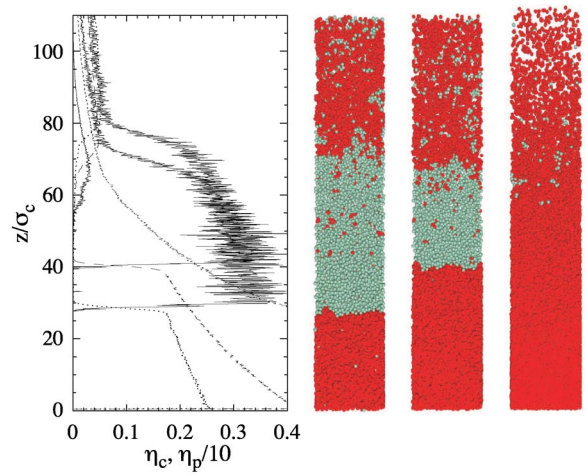

FIG. 2 (color online). Same as Fig. 1, but obtained from MC simulations, and interchanged axes. The (intermediate) case $\sigma_c/\xi_c = 0.08$ is omitted for clarity. Shown are colloid profile, $\eta_c(z)$ (solid lines), polymer profiles $\eta_p(z)$, ($\sigma_c/\xi_c = 0.06$, dotted line; 0.1, long dashed line; 0.2, short dashed line) as a function of height z/σ_c. The snapshots display particle configurations of colloids (light green) and polymers (dark red) for $\sigma_c/\xi_c = 0.06, 0.1, 0.2$ (from left to right).

the chemical potentials μ_c and μ_p, the three competing phases are a high μ_p gas phase (G), a phase containing a liquid slab at the bottom and a gas phase on top (LG), and finally the stacked gas-liquid-gas (GLG) phase. The grand potentials of these various phases have bulk contributions from the slabs, and different interfacial contributions involving the various interfacial tensions associated with the wall-fluid interface ($\gamma_{\rm wf}$) at the bottom as well as with the liquid-gas interface(s) ($\gamma_{\rm lg}$). In the GLG case let z_1 and z_2 denote the altitudes of the lower and upper liquid-gas interfaces; let $\Phi_\alpha(z) \equiv \Phi_\alpha[\rho_c(z), \rho_p(z)]$ denote the free energy per unit volume of the bulk liquid and gas phases ($\alpha = l$ or g), as calculated for each altitude from the LDA density profiles (these free energy densities contain now both $F_{\rm exc}$ and $F_{\rm id}$). The grand potential per unit (horizontal) area is then written as the sum of bulk and surface contributions

$$\Omega = \int_0^{z_1} \Phi_g(z)dz + \int_{z_1}^{z_2} \phi_l(z)dz + \int_{z_2}^{L} \Phi_g(z)dz + \gamma_{\rm wf}[\rho_c(0), \rho_p(0)] + \gamma_{\rm lg}[\rho_c^l(z_1) - \rho_c^g(z_1)] + \gamma_{\rm lg}[\rho_c^l(z_2) - \rho_c^g(z_2)]. \quad (3)$$

The three interfacial tensions appearing in Eq. (3) are calculated for the colloid and polymer densities at the three interfaces. The values of the interfacial tension for the liquid-gas interface are taken from the results of the nonlocal DFT [15], which have been shown to be very accurate for the AOV model [16]. For the wall-fluid interfacial tension $\gamma_{\rm wf}$, we used the scaled-particle result [17]. The grand potential functional (3) was evaluated with the LDA solutions for ρ_c and ρ_p. Calculations, based on expressions similar to (3), but involving only one or two interfaces, were carried out for the G and GL phases. The resulting grand potentials were then compared to determine the stable phase as a function of μ_c and μ_p. The resulting phase diagram for a mass ratio $m_p/m_c = 0.235$ is shown in Fig. 3. The floating liquid (GLG) phase is seen to be stable in a triangular region sandwiched between the G and LG phases. The three phases coexist at a triple point, below which the G and LG phases coexist along a line which terminates at a critical point. Compared to the bulk coexistence curve (i.e., in the absence of gravity) in the (μ_c, μ_p) plane, the phase diagram is seen to be shifted to larger values of μ_p, due to the action of gravity. The floating liquid phase arises from a delicate balance between gravity and interfacial tensions. The stability region of the GLG phase shrinks when the mass ratio decreases (in particular, it would be totally absent if polymer sedimentation were neglected altogether). In the limit of weak gravity, the interfacial contributions to the grand potential become negligible compared to the bulk contributions in Eq. (3). Yet the topology of the phase diagram remains unchanged, as illustrated by the inset in Fig. 3.

We have investigated the influence of polymer nonideality using a stepfunction repulsion between polymers with range σ_p and height ϵ [18]. Already relatively small values of $\beta\epsilon$ (e.g., $= 0.25$) have a pronounced effect on

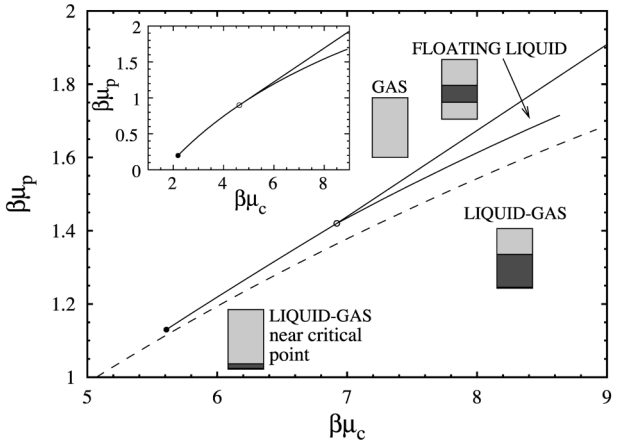

FIG. 3. The phase diagram of the AOV model under gravity as a function of the chemical potentials μ_c and μ_p, calculated within the LDA for $m_p/m_c = 0.235$, $q = 1$, and $\sigma_c/\xi_c = 0.06$. Three phases are stable: gas, floating liquid, and liquid-gas; these are sketched as cuvettes where liquid appears dark and gas appears light. Shown are the binodals (full lines), the triple point (open circle), and the liquid-gas critical point (full circle). Also shown is (part of) the bulk liquid-gas binodal (dashed line). Note that at phase coexistence the system will phase-separate *laterally*, i.e., build a vertical (curved) interface. The inset shows the result for the phase diagram for the same parameters, but in the limit of small gravity $\sigma_c/\xi_c \to 0$ and large container height $L/\sigma_c \to \infty$. The LG phase boundary is identical to the bulk binodal.

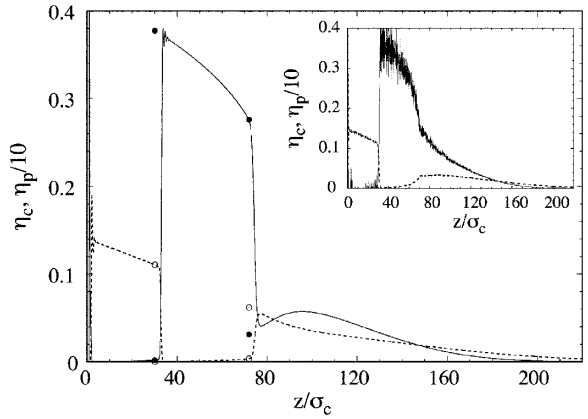

FIG. 4. Scaled density profiles of colloids (full line) $\eta_c(z)$ and polymers (dashed line) $\eta_p(z)$ versus altitude, z/σ_c, as obtained from FMT for hard spheres and nonideal polymers with $\beta\epsilon = 0.25$, mass ratio $m_p/m_c = 0.375$, size ratio $q = 1$, and inverse gravitational length $\sigma_c/\xi_c = 0.08$. Also indicated are the density jumps according to LDA for colloids (full symbols) and polymers (open symbols). The inset shows the corresponding results from MC simulation.

the location of the gas-liquid binodal [19]. Despite quantitative changes, we find the floating liquid phase to remain stable, as illustrated by the density profiles in Fig. 4. Using colloidal rods rather than polymer coils as depletant agents offers additional freedom to tune particle masses in experiments. We model such a system with colloidal hard spheres and stiff colloidal rods of length l_r and vanishing thickness [20]. Density profiles (not shown) obtained from LDA for the size ratio $l_r/\sigma_c = 1$ and a mass ratio of $m_r/m_c = 0.048$ point to the existence of the floating liquid phase.

In conclusion, DFT and MC simulations show the existence of a novel layered structure of sedimentation profiles in colloid-polymer and related mixtures. This structure demonstrates the existence, over a limited range of polymer-to-depletant mass ratios, of a floating liquid phase sandwiched between two gas slabs, the lower of which has almost vanishing colloid concentration, despite the fact that the colloidal particles are heavier than the (equal-sized) depletant particles. The required (buoyant) mass ratios might be achievable by density matching the colloidal particles to the solvent. In the case of polymer depletant, the required mass ratios are large, in view of the fact that the fractal polymer coils have a much lower bare mass than the compact colloidal particles. Using colloidal rods as depletants should render this problem less severe. The origin of the floating liquid is very different from that found in a one-component system with reentrant *bulk* phase behavior [21]. In the present case, the bulk phase diagram is fairly standard; nevertheless, there is the possibility that a sedimentation path crosses the binodal twice (see inset of Fig. 1). The stability region of the resulting floating liquid phase in the phase diagram is then determined by the balance between bulk, gravitational, and interfacial contributions to the free energy. This scenario is generic for a wider range of binary mixtures undergoing phase separation in the bulk. Provided mass densities of both phases involved (not necessarily fluids) can be tuned to coincide at one statepoint, the phase towards which the binodal bends in the phase diagram spanned by both chemical potentials will float between slabs of the other phase.

This work was carried out during JPH's tenure of the Kramers Chair of the University of Utrecht. The work of MS is part of the research program of FOM, that is financially supported by the NWO. We acknowledge support by the SFB-TR6 of the DFG.

*On leave from Institut für Theoretische Physik II, HHUD, Universitätsstraße 1, D-40225 Düsseldorf, Germany.

†On leave from Department of Chemistry, University of Cambridge, Lensfield Road, Cambridge CB2 1EW, UK.

[1] J. Perrin, J. Phys. **9**, 5 (1910).
[2] R. Piazza, T. Bellini, and V. Degiorgio, Phys. Rev. Lett. **71**, 4267 (1993).
[3] T. Biben and J. P. Hansen, Mol. Phys. **80**, 853 (1993).
[4] T. Biben and J. P. Hansen, J. Phys. Condens. Matter **6**, A354 (1994).
[5] A. P. Philipse and G. H. Koenderink, Adv. Colloid Interface Sci. **100**, 613 (2003).
[6] R. van Roij, J. Phys. Condens. Matter **15**, S3569 (2003); A. P. Hynninen, R. van Roij, and M. Dijkstra, Europhys. Lett. **65**, 719 (2004).
[7] H. H. Wensink and H. N. W. Lekkerkerker, Europhys. Lett. **66**, 125 (2004).
[8] S. Asakura and F. Oosawa, J. Chem. Phys. **22**, 1255 (1954); A. Vrij, Pure Appl. Chem. **48**, 471 (1976).
[9] H. N. W. Lekkerkerker *et al.*, Europhys. Lett. **20**, 559 (1992).
[10] M. Dijkstra, J. M. Brader, and R. Evans, J. Phys. Condens. Matter **11**, 10079 (1999).
[11] T. Biben, J. P. Hansen, and J. L. Barrat, J. Chem. Phys. **98**, 7330 (1993).
[12] Y. Rosenfeld, Phys. Rev. Lett. **63**, 980 (1989).
[13] M. Schmidt *et al.*, Phys. Rev. Lett. **85**, 1934 (2000).
[14] See, e.g., I. Bodnár, W. D. Oosterbaan, J. Chem. Phys. **106**, 7777 (1997) for experimental results. The tielines in the (η_c, η_p) plane change slope as a function of statepoint implying a curved binodal in the (μ_c, μ_p) plane via (2).
[15] J. M. Brader, *et al.*, J. Phys. Condens. Matter **14**, L1 (2002).
[16] R. L. C. Fink and R. Horbach, J. Chem. Phys. **121**, 3253 (2004).
[17] P. P. F. Wessels, M. Schmidt, and H. Löwen, J. Phys. Condens. Matter **16**, L1 (2004).
[18] M. Schmidt, A. R. Denton, and J. M. Brader, J. Chem. Phys. **118**, 1541 (2003).
[19] R. L. C. Vink (unpublished).
[20] P. Bolhuis and D. Frenkel, J. Chem. Phys. **101**, 9869 (1994).
[21] J. Dzubiella, H. M. Harreis, C. N. Likos, and H. Löwen, Phys. Rev. E **64**, 011405 (2001).